Relationship between the Weldability and the Process Parameters for Laser-TIG Hybrid Welding of Galvanized Steel Sheets

Cheolhee Kim[1], Woongyong Choi[2], Jeonghan Kim[1] and Sehun Rhee[3]

[1]*Advanced Joining Technology Team, Korea Institute of Industrial Technology, Incheon 406-130, Korea*
[2]*Digital Media Business, Samsung Electronics, Suwon 443-742, Korea*
[3]*School of Mechanical Engineering, Hanyang University, Seoul 133-791, Korea*

In the lap welding of zinc-coated steel, porosity formation is one of most significant weld defects. It is caused by zinc vapor generated between the steel sheets. Various solutions have been proposed in the past but development of more effective method remains a valuable subject to be investigated. In this study, laser-TIG hybrid welding was applied to the lap welding of zinc-coated steel without a gap. The weld defects could be eliminated by laser-TIG hybrid welding, as the leading TIG arc partially melted the upper sheet, and the coated zinc on the lapped surfaces were vaporized or oxidized before the trailing laser irradiated on the specimen.

Optimization of the process parameters for laser-arc hybrid welding process is intrinsically sophisticated because the process has three types of parameters–arc, laser and hybrid welding parameters. In this paper, the relationship between weldability and the process parameters of the laser beam-arc distance, welding current and welding speed were investigated using a full factorial experimental design. Weld quality was evaluated using the weight of the spatter, as porosity formation is a major weld defect in the lap welding of zinc-coated steel sheets. It was found that the weld quality was increased as the laser beam-arc distance and welding current increased, and that this decreased as welding speed increased. [doi:10.2320/matertrans.MER2007159]

1. Introduction

Galvanized steel is widely used for car bodies due to its corrosion resistance. However, it is associated with serious problems related to the welds quality when laser welding is applied to a lap joint without gaps. These problems occur because the boiling point of zinc ($906°C$) is lower than the melting point of steel, the base material, (about $1500°C$).[1] When the laser is irradiated, the galvanized layer between the steel sheets is vaporized before the base material is melted. The zinc vapor under pressure explodes through the relatively weak melting pool. The expulsion causes numerous weld defects such as spattering, blowholes on the weld surface and porosity formation inside the welds. The blowholes and pores resulting from the aforementioned process influence the mechanical characteristics, leading to defective welds. Accordingly, they should be prevented in advance.

Various studies have focused on the prevention of defects that result from the laser welding of a galvanized lap joint, and investigations for more effective methods are in progress. The methods that have been developed thus far include the securing of a path to vent the zinc vapor by providing gaps in the lap joint of the base materials, welding after removing the galvanized layer using mechanical or chemical methods, controlling the formation of key holes using a pulse laser, and welding to remove the galvanized layer using two laser beams.[2–6] Among these methods, the method that utilizes gaps in the joint is widely used in the field. However, it is not easy to control the gap. The other methods are not used due to the low productivity associated with those methods.[7]

The laser-arc hybrid welding process applies laser welding power and arc welding power simultaneously to compose a single weld, utilizing the advantages of both methods. It allows preheat and post heat treatments on the welds through the arrangement of the laser and arc.[8–10] As the lap welding of the galvanized steel plate does not need filler material, Gu and Miller reviewed the applicability applying laser-TIG hybrid welding and explained the welding phenomenon through a qualitative hypothesis.[11] It is not easy to optimize the process, as there are many process variables; laser–TIG hybrid welding inherently incorporates variables for the laser, arc and hybrid process. Thus, the effects of the process parameters are not fully understood for the laser–TIG hybrid welding on a galvanized steel plate.

Therefore, in this study, the influences of the welding parameters on the weld quality are investigated using a full factorial experimental design. The laser beam-arc distance, the welding current and the welding speed are utilized as the control parameters.

2. Experimental Setup and Procedure

The steel plates used in this study were SGCD1 galvanized steel plates specified in JIS G 3302, the mechanical properties and composition of which are shown in Table 1. Both sides are galvanized with $54 \, g/m^2$ zinc, and the width, length, and
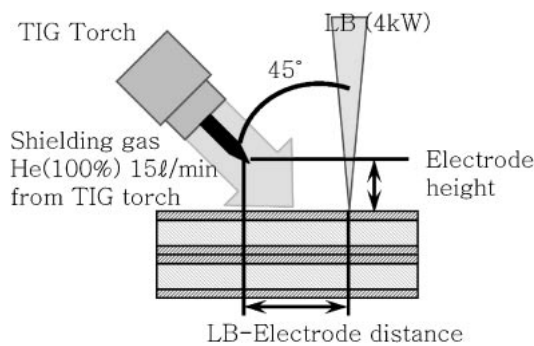
Table 1 Properties of SGCD1 steel used.

Mechanical properties	
Yield strength (MPa)	147
Tensile strength (MPa)	292
Elongation (%)	48
Chemical composition (mass%)	
C	0.0028
Si	0.009
Mn	0.129
P	0.0079
S	0.0097
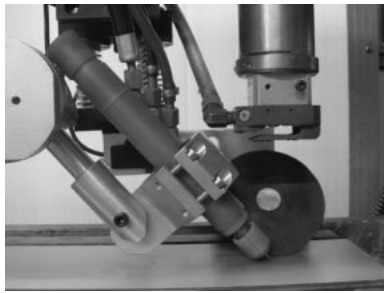
(a) Photo of laser-TIG hybrid head
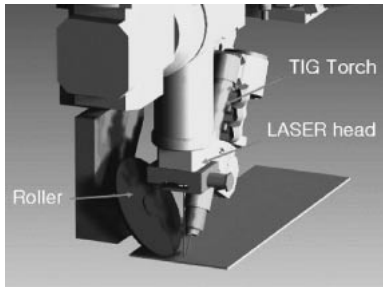
(b) Schematic diagram of laser-TIG hybrid head

(c) Schematic diagram

Fig. 1   Experimental setup for hybrid welding.

Table 2   Welding conditions used in experiments.

Specimen	SGCD1 (300 mm × 100 mm × 1 mm)
Laser power	4 kW
Shielding gas	He 100%(15 L/min)
Electrode diameter	1.6 mm
Torch angle	45 deg.
Joint	Lap joint

thickness of the plate were 100 mm, 300 mm and 1 mm, respectively. The thickness of the zinc coating was approximately 50 μm.

In the experiment, a CO_2 laser with a rated continuous wave output of 12 kW was used. The laser light was delivered by a 50 mm concave mirror with a focal length of 250 mm to the surface of the base metal. The diameter of the laser spot was approximately 0.4 mm at the focal point. An inverter TIG power source with a rated output of 300 A and 1.6 mm diameter tungsten electrode were used for the TIG welding. All trials were conducted at DC electrode-negative (DCEN) and with a constant current configuration. The experimental setup, including a customized hybrid welding head and the definitions of the welding parameters, is shown in Fig. 1. A perpendicularly irradiated laser beam was focused on the surface of the base material, and a TIG torch was installed at an inclination degree of 45 degrees. Pure helium was used as the shielding gas and was supplied through the TIG torch nozzle at 15 L/min. The workpiece was pressed and fixed without a gap using a devised guide-roller which is made up of a wheel and spring system and attached to the hybrid welding head. The fixed welding variables for the experiment

are summarized in Table 2. The welding phenomena were recorded with the frame rate of 1500 frame/s by using a high-speed camera.

With the fixed laser output, the relationship between the process variables and weldability was evaluated by changing the laser beam-arc distance, welding current and welding speed. Here, laser-TIG hybrid welding was applied, with TIG leading laser.

3.   Weld Defects and Evaluation

In order to identify the weld defects in laser lap welding on the galvanized steel sheets, the laser welding was implemented on galvanized steel plates and non-galvanized steel plates with a 4 kW output at 3.0 m/min.

Figure 2 shows the top surface and bottom surface of welds that resulted from (a) bead-on-plate welding performed on a piece of the galvanized steel sheet without overlapping, (b) lap joint welding without a gap on galvanized steel sheets, and (c) lap joint welding without a gap on non-galvanized steel sheets. In the lap joint welding without a gap on galvanized steel sheets, much spatter was generated during the welding process, creating large blowholes on the weld surface. On the other hand, with the lap joint welding without a gap on non-galvanized steel sheets as well as with the bead-on-plate welding, sound welds were formed without defects both on the top and bottom surfaces. Thus, weld defects in lap joint welding without a gap on galvanized steel sheets resulted from the galvanized layer on the lapped surfaces.

Figure 3 shows the top surface, a longitudinal cross-section and a transverse cross-section of the welds that resulted from lap joint welding without a gap on galvanized steel sheets. There were weld defects inhibiting bead continuity throughout the welds. The representative weld defects were blowholes and porosities. Ono *et al.* explained the cause of these defects as follows: when the upper base metal is melted by the irradiation of the laser, zinc on the lapped surfaces is vaporized at the same time because the melting temperature of the steel is higher than the vaporization temperature of the zinc. The pressure of the zinc vapor increases, and it then explodes through the melting pool, which has a relatively low pressure.[3] Figure 4 shows high-speed images of the laser-autogenous welding of zinc-coated steel sheets.

It was found that the shape of the melting pool rapidly changes due to the increase in the pressure of the zinc vapor inside the melting pool and the subsequent zinc vapor bursting out with spattering. This quantitatively shows the cause of the aforementioned defects.
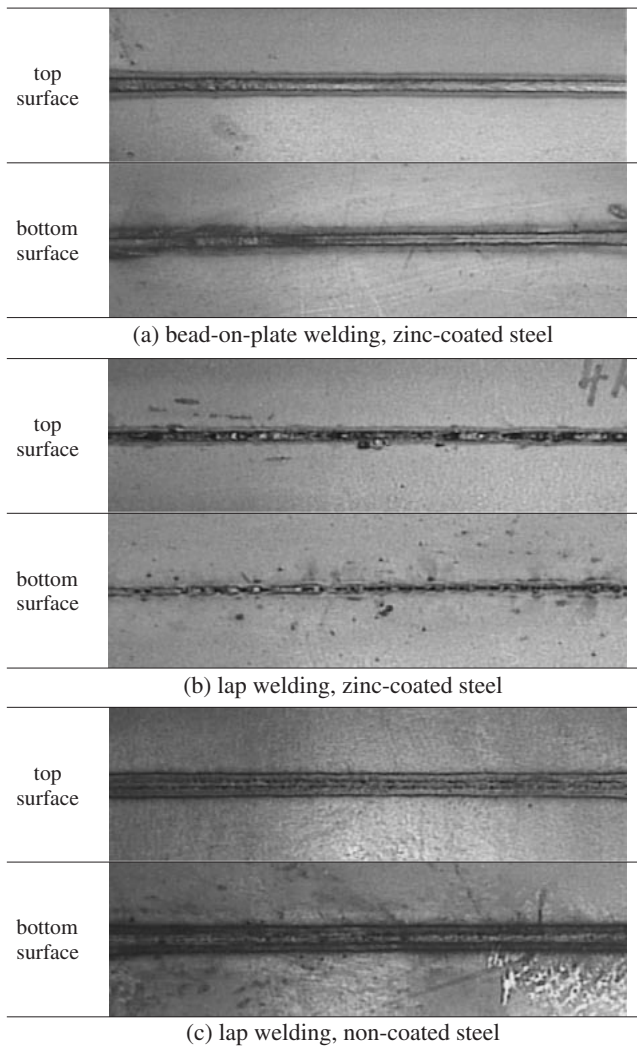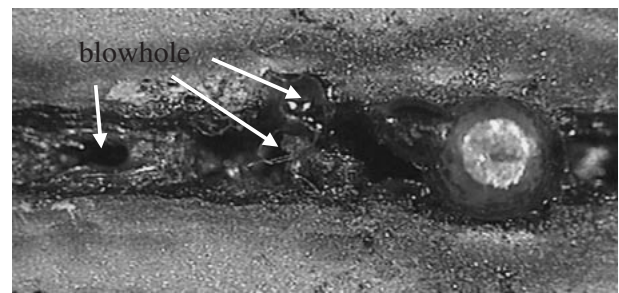
(a) bead-on-plate welding, zinc-coated steel

(b) lap welding, zinc-coated steel

(c) lap welding, non-coated steel

Fig. 2   Bead Surfaces for autogenous laser welding of zinc-coated and non-coated steel sheets.

(a) top surface

(b) longitudinal cross-section

(c) transverse cross-section

Fig. 3   Weld defects for autogenous laser lap welding of zinc-coated steel.

The weld beads after CO_2 laser-TIG hybrid welding were also examined with the welding speed of 3.0 m/min. Cross-sections of the welds on which TIG leading laser-TIG hybrid welding was conducted are shown in Fig. 5. Sound welds without porosity formed over the entire weld bead, and the bead has excellent consistency along the longitudinal direction, as shown in the longitudinal cross-section shown in Fig. 5(b). From the transverse cross-section shown in Fig. 5(c), it was found that the TIG arc partially melted the upper sheet and that the laser beam melted both plates in the keyhole mode which enables a high penetration depth-to-bead width ratio.
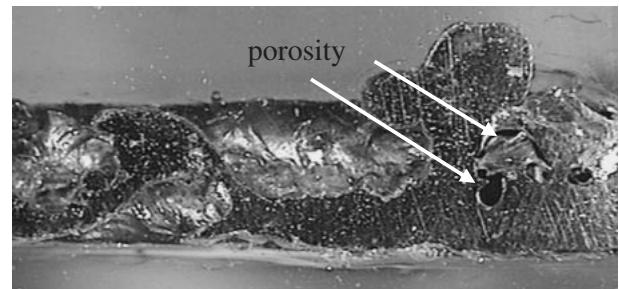
The high-speed images in Fig. 6 show that the molten pool and the keyhole were stable and that no bursting occurred.

In the case of TIG bead-on-plate welding with the welding speed of 3.0 m/min, the oxidized zinc was found on the bottom surface, as shown in Figs. 7 and 8. At the same time, it was found that the zinc layer was partially removed on the bottom surface as shown in the EDS results in Fig. 9, where the EDS analysis was conducted perpendicularly to the welding direction.
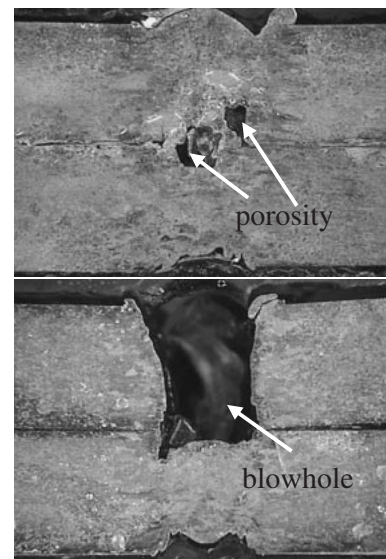
Accordingly, it is hypothesized that defects such as porosity can be prevented with an application of laser-TIG hybrid welding on galvanized steel plates. This is true for two reasons. First, just as in the method using two lasers, the leading TIG arc vaporizes zinc on the lapped surface, and the zinc vapor exhausts through the gap between the sheets before the trailing laser arrives. Second, the leading TIG arc applies heats to zinc over the melting point (419.5°C), and the melted zinc is rapidly oxidized before the trailing laser arrives. The zinc vapor can be reduced because the melting point of oxidized zinc (1975°C for ZnO) is higher than that of the iron.

As mentioned above, the most critical welding defect is porosity formation caused by spatter generation in laser-TIG hybrid welding. It was for this reason that the weight of the spatter was used as the criterion for the weld quality. The

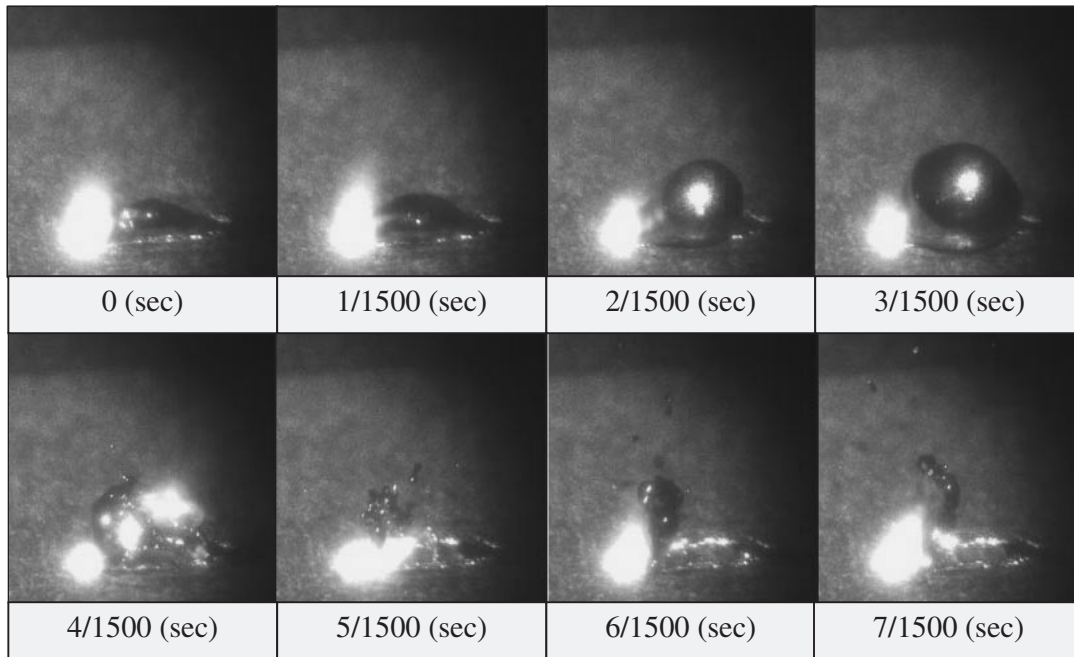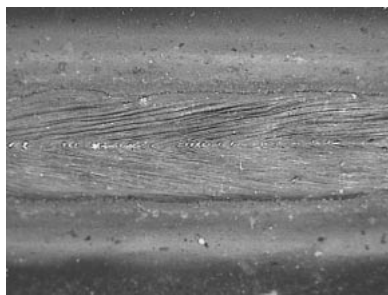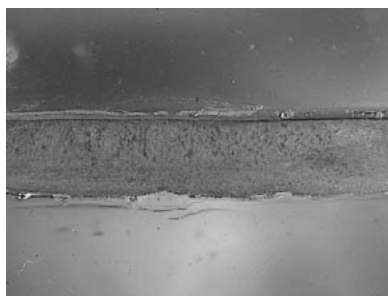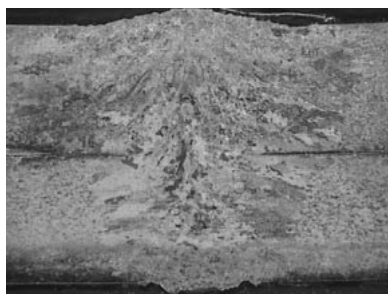| 0 (sec) | 1/1500 (sec) | 2/1500 (sec) | 3/1500 (sec) |
| 4/1500 (sec) | 5/1500 (sec) | 6/1500 (sec) | 7/1500 (sec) |

Fig. 4   High speed images for autogenous laser lap welding of zinc-coated steel sheets.

(a) top surface

(b) longitudinal cross-section

(c) transverse cross-section

Fig. 5   Cross-sectional bead shapes for CO2 Laser-TIG hybrid weld (100 A arc current; 1 mm electrode height; 7 mm LB-electrode distance; TIG leading).

weight of the spatter was assumed by measuring the weight reductions of the specimen before and after welding.

Figure 10 shows the results of radiographic tests on samples with different levels of measured weight reduction. Using the radiographic results, the ratio of the pore area to the total area of the welds was calculated. Its relationship with weight of the spattered material is shown in Fig. 11. It was confirmed that there is a definite correlation between the amount of spatter and defects in the welds.

4.   Evaluation of Welding Parameters

4.1   Height of electrode and its damage

In TIG welding in electrode negative mode, the electrode tips are ground at a fixed angle in order to increase the stability of the process by concentrating. Because changes in the electrode geometry can significantly influence the weld bead shape and size, consistent electrode geometry should be maintained. As a constant current power source was used in the experiments, the height of the tip was proportional to the welding voltage. Therefore, the welding voltage was measured and adopted as the criterion for tip deterioration.

Figure 12 shows the welding voltage waveforms measured according to the number of welding trials at each electrode height. Figure 13 shows the damage to the welding electrode. During the first experiment, there was a rapid increase in the welding voltage at an electrode height of 0.4 mm while the voltage was maintained as nearly constant throughout the subsequent trials. As shown in Fig. 13(b), the electrode was blunted after the first trial. When the height of the electrode was 1.0 mm, the electrode was blunted after the second welding trial and a rapid increase in the voltage was found in the voltage waveform for the second trial. When the height of the electrode was 2.0 mm, it was not blunted even after ten experiments, and there was no rapid rise in the voltage waveforms.

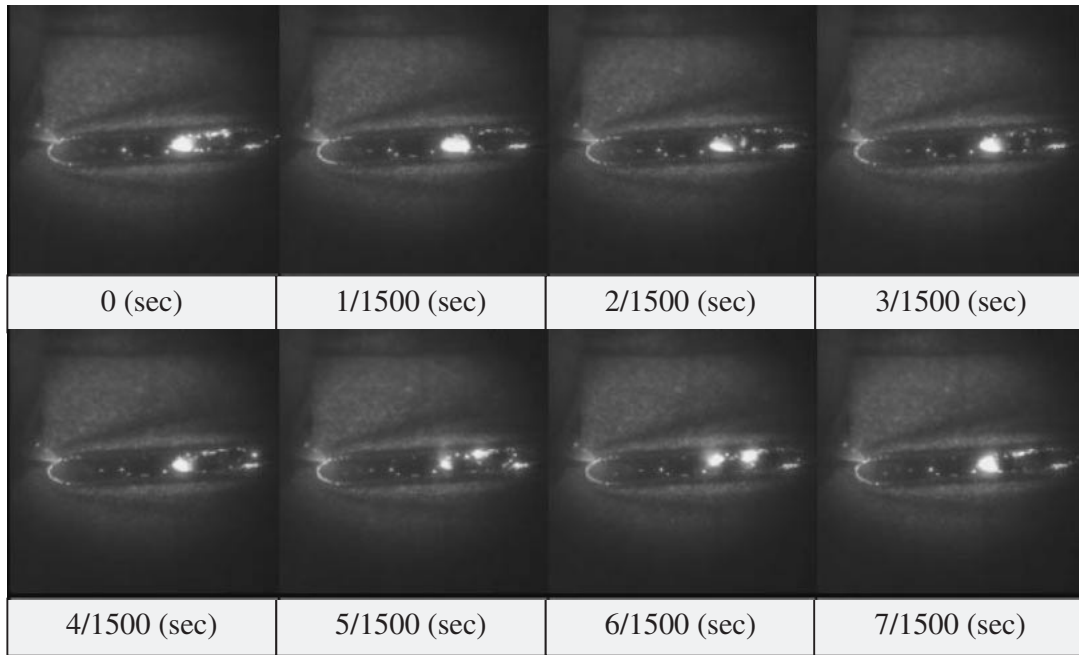| 0 (sec) | 1/1500 (sec) | 2/1500 (sec) | 3/1500 (sec) |
| 4/1500 (sec) | 5/1500 (sec) | 6/1500 (sec) | 7/1500 (sec) |

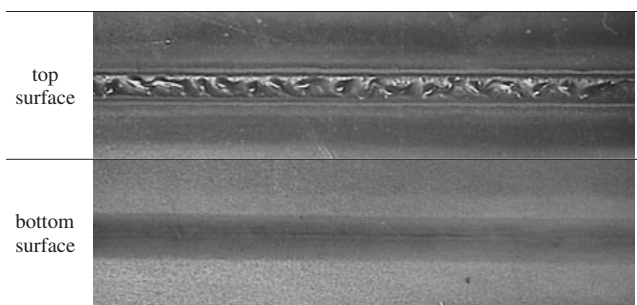Fig. 6   High speed images for CO2 Laser-TIG hybrid lap welding of zinc-coated steel sheets.

Fig. 7   Bead Surfaces for TIG bead-on-plate welding of zinc-coated sheets (100 A arc current; 1.0 mm electrode height).
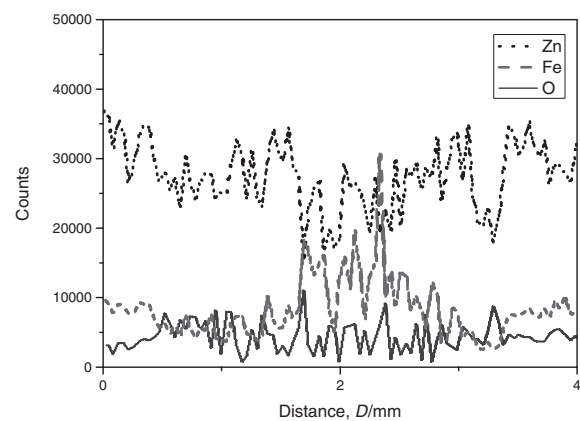

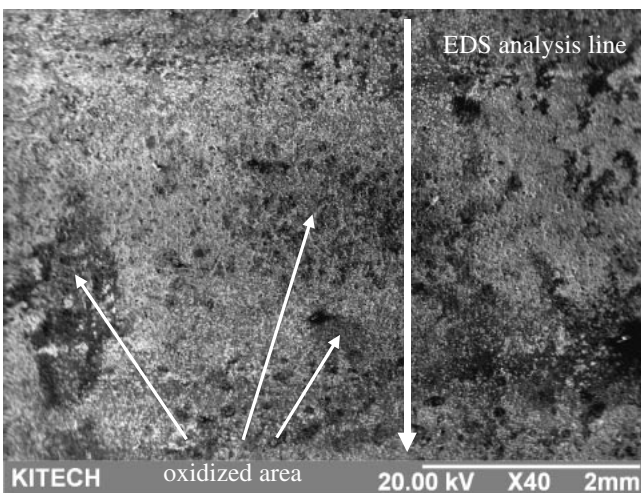Fig. 9   EDS results for bottom surface for TIG bead-on-plate welding of zinc-coated sheets.

Fig. 8   SEM images for bottom surface for TIG bead-on-plate welding of zinc-coated sheets.

4.2   Effects of Welding Current, Distance between Laser Beam and Electrode, and Welding Speed

The height of the electrode was fixed at 2 mm in order to avoid having to replace the electrode frequently. The effects of the welding current, the distance between laser beam and the electrode, and the welding speed on the amount of spatter was investigated. As shown in Table 3, each factor has three levels and welding was performed three times for each of the 27 combined conditions. The analysis of variance (ANOVA) results for the main effects (A, B, C), the interaction effects between two factors (A*B, B*C, C*A) and the error term(ERROR) are shown in Table 4. F_0 is the F value calculated from the F distribution which is determined by the number and degrees of freedom of the factors.[12] When the P-value, P is less than 0.05, the effect of the factor is statistically significant at a significance level of $\alpha = 0.05$.

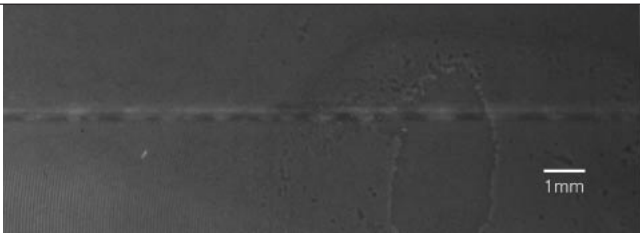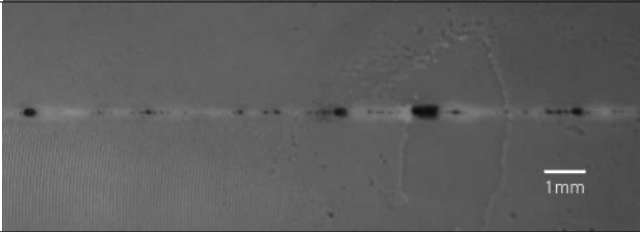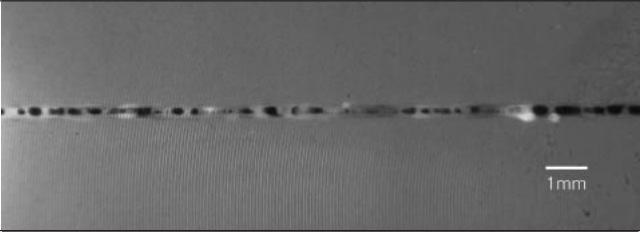Regarding the main effects for each factor, the main effects
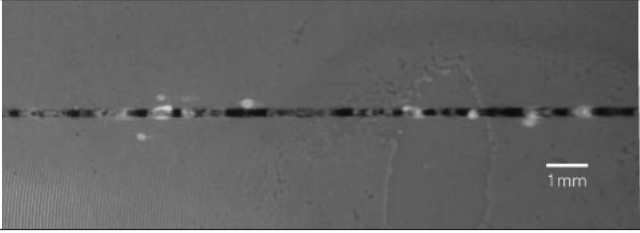
case No.	RT result	spatter weight (g)
1		0.1
2		0.4
3		0.8
4		1.4

Fig. 10   Radiation test results for various spatter weights.
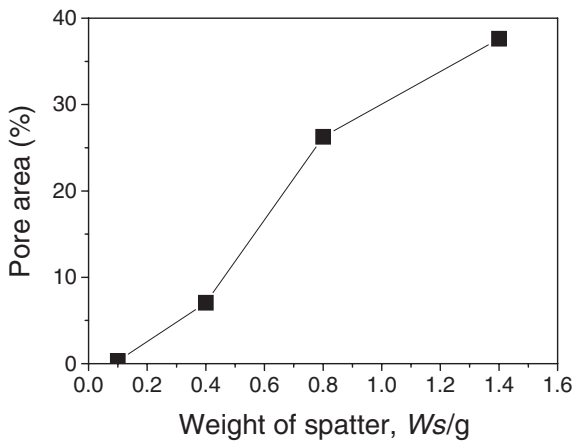
Fig. 11   Relationship between weight of spatter and pore area.

Table 3   Control factors and their levels for the full factorial design.

Factor	Level		
	1	2	3
A. Welding current (A)	80	100	120
B. LB-electrode distance (mm)	5	7	9
C. Travel speed (m/min)	2.5	3.0	3.5

Table 4   ANOVA results for the full factorial experiments with Table 3.

Source	Degree of freedom	Sum of squares	Mean square	F_0	P
A	2	0.3499	0.1749	17.88	0.001
B	2	0.0402	0.0201	2.06	0.190
C	2	0.1252	0.0626	6.40	0.022
A*B	4	0.0084	0.0021	0.21	0.923
B*C	4	0.0235	0.0059	0.60	0.674
C*A	4	0.0531	0.0133	1.36	0.33
Error	8	0.0783	0.0098		
Total	26	0.6785			

of welding current and the welding speed are significant at a significance level of $\alpha = 0.05$, as the P-value is under 0.05 in the cases of A and C. The main effect of the distance between the laser beam and the electrode (B) and the interaction effects between the two factors (A*B, B*C, C*A) have P-values over 0.05, which implies that they are not statistically significant. The P-value for the main effect of the distance between the laser beam and the electrode is significantly smaller than the values for the interaction effects. Accord-
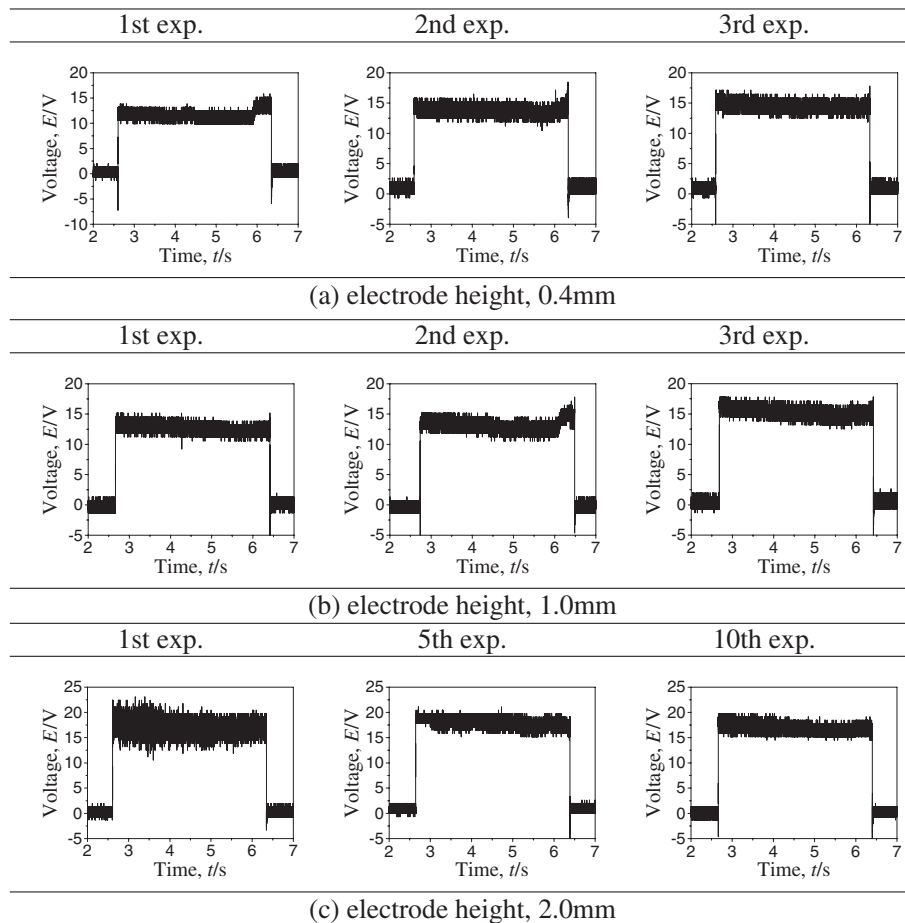
Fig. 12 Variation of welding voltage waveforms for each electrode height (100 A arc current; 5 mm LB-electrode distance; 3 m/min travel speed).

ingly, to identify the effects of the main factors on the amount of spatter ignoring the influence of interaction, the average amounts of spatter generated at the levels for each factor are shown in Fig. 14.

As shown in Fig. 14, less spatter was created as the welding current and distance between laser beam and electrode increased, and more spatter was created as the welding speed increased.

Laser-TIG hybrid welding can reduce the defects of the lap joint welds for galvanized steel sheets, as heat caused by the leading arc causes zinc on the lapped surfaces to vaporize or oxidize before the trailing laser arrives. Therefore, if the welding current is higher, it will increase the heat input by the arc, and the zinc layer can be more widely removed. If the distance between the laser beam and the electrode were increased, there would be enough time for exhausting the vaporized zinc and for the oxidization of the melted zinc. Thus, less spatter would be created.

On the other hand, with an increase in the welding speed, the heat input for unit length by the TIG arc was reduced; consequently, the zinc layer is insufficiently removed. Moreover, an increase in the welding speed reduces the time interval between the arc heating and laser irradiation, making the time insufficient for zinc vapor to be exhausted or oxidized, even for identical distances between the laser beam and electrode.

5.   Conclusion

In this study, the influences of the welding process parameters on the weldability were investigated for laser-TIG hybrid welding of galvanized steel sheets. The conclusions of this study can be summarized as follows:
(1) When TIG preceding laser-TIG hybrid welding is applied to the lap joint welding of galvanized steel sheets without a gap, good welds without blowholes and bubbles can be obtained. Zinc vaporization and oxidization by heat of the preceding arc before the following laser arrives may remove the defects of the welds.
(2) Porosity is the main defect during laser lap welding of galvanized steel sheets. The amount of spatter was adopted as the criterion to evaluate the weldability, as the pore area is in proportion to the amount of spatter, which was approximated using the weight reduction of the specimen before and after welding.
(3) During laser-TIG hybrid welding, the electrode height should be maintained over 2.0 mm to prevent damage to the electrode tip.
(4) When the weldability was evaluated according to the welding current, travel speed and distance between laser beam and the electrode at a fixed electrode height of 2.0 mm, the main effects of the welding current, and the welding speed were statistically significant. A lower speed welding and a higher welding current showed better weldability.

(a) before welding

(b) 0.4mm (after 1st trial)

(c) 1.0 mm (after 2nd trial)

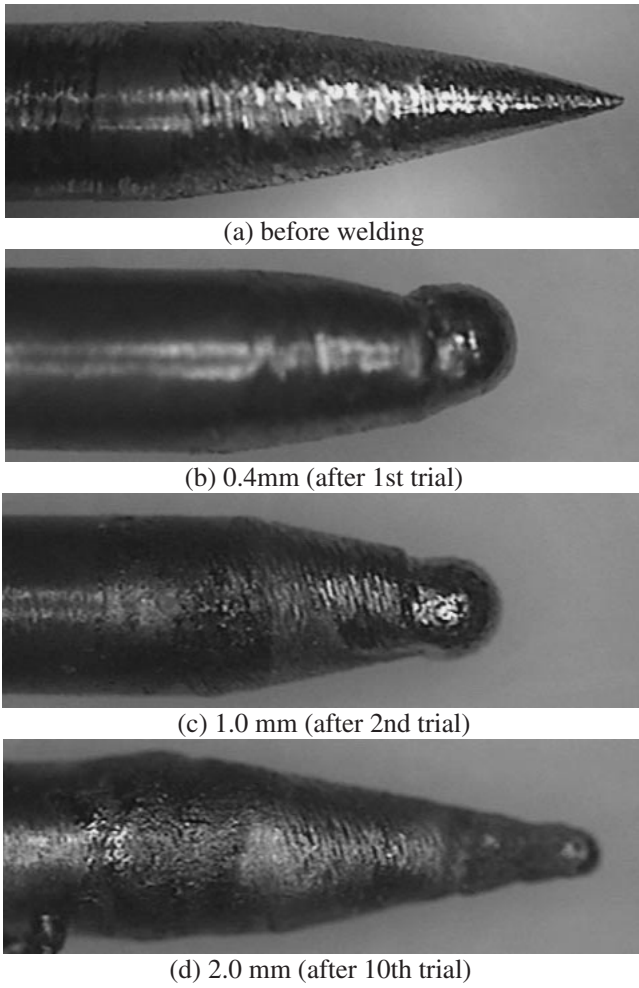(d) 2.0 mm (after 10th trial)

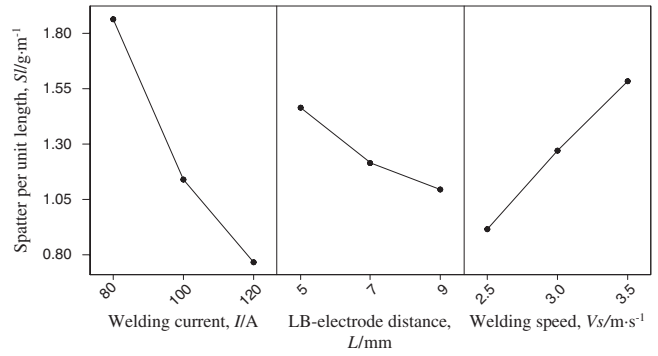Fig. 13   Deterioration of electrode tip for various electrode heights after experiments.

Fig. 14   Main effects of control parameters on weight of spatter.

REFERENCES

1) G. S. Brady and H. R. Clauser: *Materials Handbook*, 12th ed., (McGraw-Hill, New York, 1989) pp. 896–902.
2) R. Akhter, R. W. M. Steen and D. Cruciani: Proceedings of the 5th Int. Conf. on Lasers in Manufacturing (1988) pp. 195–206.
3) M. Ono, S. Kaizu, M. Ohmura, M. Kabasawa and K. Mori: Q. J. Jpn. Weld. Soc. **15** (1997) 438–444.
4) Y.-F. Tzeng: Weld. J. **78** (1999) 238s–244s.
5) M. M. S. Gualini: International Congress on Applications of Laser and Electro-Optics (ICALEO'2003), LMP Section A (2003) pp. 274–284.
6) M. G. Forrest and F. Lu: International Congress on Applications of Laser and Electro-Optics (ICALEO'2004), Laser Welding and Brazing Section (2004) pp. 112–119.
7) M. M. S. Gualini: International Congress on Applications of Laser and Electro-Optics (ICALEO'2001), Section C (2001) Paper No. P511.
8) W. M. Steen, M. Eboo and J. Clarke: 4th International Conference on Advances in Welding Processes Proceedings (1978) pp. 257–265.
9) N. Abe and H. Hayashi: Weld. Int. **16** (2002) 94–98.
10) C. Bagger and F. O. Olsen: J. Laser Appl. **17** (2005) 2–14.
11) H. Gu and R. Miller: International Congress on Applications of Laser and Electro-Optics (ICALEO'2001), Section A (2001) Paper No. 304.
12) J. L. Devore: *Probability and Statistics for Engineering and the Sciences*, 3rd ed., (Brooks/Cole Publishing Co., Pacific Grove, CA, 1991) pp. 371–379.